jet INTL JOURNAL OF ELECTRONICS AND TELECOMMUNICATIONS, 2026, VOL. 72, NO. 2, PP. 1–9
Manuscript received January 13, 2026; revised April 2026. doi: 10.24425/ijet.2026.157907

A comparative performance analysis of phase configuration algorithms in Near-Field for Multi-User LIS-Aided UAV systems

Truong Anh Dung, Pham Thanh Hiep, Nguyen Thu Phuong, and Le Hai Nam

***Abstract*—Large intelligent surfaces (LIS) are a key 6G technology, but extremely large antenna arrays (ELAA) necessitate near-field (NF) operation, challenging conventional far-field (FF) beamforming. This paper addresses NF multi-user (MU) beamforming in a LIS-aided Unmanned Aerial Vehicle (UAV) relay system. We develop and compare two distinct phase configuration algorithms for multi-beam NF focusing: a low-complexity Grouped Beamforming heuristic and a Grey Wolf Optimizer (GWO) Beamforming metaheuristic. Performance, including Average Array Gain, Average Minimum Array Gain, their Cumulative Distribution Functions, and computational complexity, is evaluated via Monte Carlo simulations against baseline methods. Both proposed algorithms significantly outperform baselines. GWO Beamforming especially ensuring fairness under high user loads, but incurs a considerable computational cost. Conversely, Grouped Beamforming offers a practical real-time solution. Our findings illuminate the critical performance-complexity trade-offs guiding algorithm selection for NF MU LIS-UAV deployments.**

***Keywords*—Large Intelligent Surface (LIS); Near-Field Beamforming; Multi-User; UAV Relay; 6G; Grouped Beamforming; Grey Wolf Optimizer (GWO)**

I. Introduction

SIXTH -generation (6G) wireless communication systems are expected to provide ultra-high data rates, massive connectivity, and ultra-low latency to support future applications such as virtual/augmented reality (VR/AR) and the Internet of Everything (IoE) = [1], [2]. To achieve these ambitious goals, new technologies like Extremely Large-Scale Antenna Arrays (ELAA) or Large Intelligent Surfaces (LIS) are being extensively researched = [3], [4]. LIS, with its ability to intelligently control radio waves, promises to reshape the communication environment to enhance system performance = [5]. Concurrently, the use of Unmanned Aerial Vehicles (UAVs) as aerial relay stations offers superior advantages in flexibility, rapid deployment, and on-demand coverage, especially in temporary or disrupted network scenarios = [6], [7]. The integration of LIS into UAV relay systems (LIS-Aided UAV Relay Systems) has emerged as a powerful solution, combining the environment-reconfiguring capabilities of LIS with the mobility of UAVs to efficiently support multiple users = [8].

A fundamental change when using LIS or ELAA is the system's operational region = [4]. With extremely large antenna apertures, users are highly likely to be in the radiative near-field (NF) region, also known as the Fresnel region, rather than the traditional far-field (FF) region = [9], [10]. In the far-field, waves are assumed to be planar, and beamforming is only angle-dependent. However, in the near-field, this assumption is no longer valid; waves must be accurately modeled as spherical wavefronts = [11]. Consequently, conventional far-field beamforming techniques suffer from severe performance degradation due to phase mismatch = [10]. Conversely, near-field communication (NFC) enables a new capability called "beamfocusing," where energy can be concentrated onto a specific point in space, defined by both angle and distance = [11], [12].

The primary challenge in multi-user LIS-aided UAV systems is the design of effective multi-beamforming in the near-field scenario = [13]. This requires generating multiple focused beams simultaneously to multiple users, which introduces significant inter-user interference (IUI) due to the complex characteristics of near-field beams = [14]. Furthermore, the mobility of the UAV and potential positioning errors further complicate channel modeling and beamforming design = [7]. Therefore, the optimization problem becomes extremely complex, requiring the joint optimization of active beamforming at the UAV and passive beamforming (reflection coefficients) at the LIS to maximize system performance, such as the sum-rate = [8], [15].

To address this complex and non-convex optimization problem, researchers generally follow two main approaches. The first approach utilizes domain-knowledge-based heuristics = [16]. These methods often decompose the complex problem into simpler sub-problems, such as a "two-stage heuristic approach" to separately optimize analog and digital beamformers = [12], or distributed algorithms to handle phase errors = [7]. A typical example is the 2D+1D beamforming design in = [9], where 2D far-field (angle) beamforming is combined with 1D near-field (distance) beamforming to compensate for losses. Although these heuristic methods often have low computational complexity, they may not achieve globally optimal performance = [17].

T.A. Dung, P.T. Hiep, N.T. Phuong and L.H. Nam are with Le Quy Don Technical University, No 236, Hoang Quoc Viet, Ha Noi, Viet Nam (e-mail: dungta@lqdtu.edu.vn, thanhhiep@lqdtu.edu.vn, phuong.nt@lqdtu.edu.vn, namlh@lqdtu.edu.vn).

TABLE I: Comparison with Related Work

Work	Near-Field	Multi-User	UAV-LIS	Method
= [9]	✓	×	× (LIS Only)	Heuristic (2D+1D)
= [7]	✓	×	× (UAV Only)	Phase Error Comp.
= [12]	✓	✓	×	Heuristic (Two-Stage)
= [13]	✓	✓	× (UAV Only)	3D Velocity Sensing
= [14]	✓	✓	× (LIS Only)	Beam-Training
= [16]	×	✓	× (LIS Only)	DRL
= [17]	×	✓	× (LIS Only)	GWO (For FF Phase Shift)
= [18]	✓	×	× (LIS Only)	GWO (For LIS Placement)
= [21]	✓	×	×	AI (Sidelobe Reduction)
= [22]	×	✓	× (UAV Only)	Trajectory Optimization
= [23]	✓	✓	× (MIMO)	Performance Analysis (SE)
= [28]	×	✓	× (UAV Only)	Trajectory Opt. (ISAC)
This Work	✓	✓	✓ **(UAV + LIS)**	**Heuristic vs. Metaheuristic**

Note: Our work is the first to provide comprehensive performance-complexity comparison of grouped heuristics and metaheuristic optimization for NF MU LIS-UAV systems.

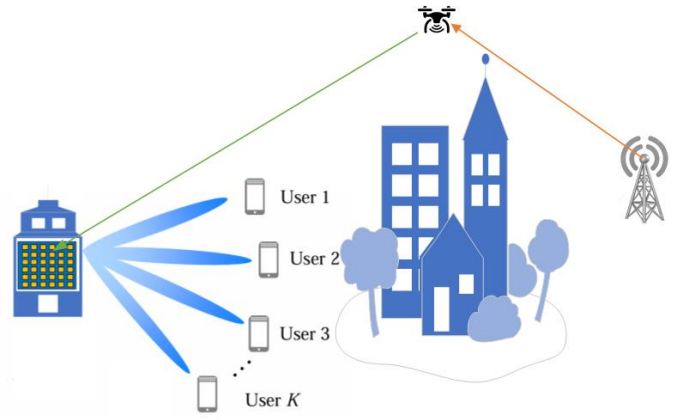

Fig. 1: System model.

The second approach applies nature-inspired meta-heuristic algorithms, which are highly effective in solving complex, non-linear optimization problems = [18]. Among them, the Grey Wolf Optimization (GWO) algorithm has garnered significant attention = [19]. GWO simulates the social hierarchy and hunting behavior of grey wolves, demonstrating faster convergence and more effective avoidance of local optima compared to other meta-heuristics like Genetic Algorithms (GA) = [20], [21]. GWO has been proven effective in optimizing antenna array beam patterns, reducing Sidelobe Level (SLL) = [20], and solving joint trajectory and beamforming optimization problems in UAV systems = [8], [22].

Based on the literature analysis above = [3], [23], [24], several critical research gaps remain. First, most research on near-field beamforming for LIS/UAVs focuses on single-user scenarios. The design of multi-beamforming for multi-user scenarios in the near-field, especially the joint optimization of LIS and UAV, remains underexplored = [14]. Second, spatial non-stationarity across extremely large LIS is a major challenge in the near-field [11], yet many current algorithms overlook this characteristic. Third, while grouped heuristics = [12] offer low complexity, they are often sub-optimal solutions = [17]. Conversely, powerful methods like Deep Reinforcement Learning (DRL) = [16] or meta-heuristics = [8] come with a significant computational burden, making them difficult to apply in real-time. Finally, to the best of our knowledge, the specific application of GWO to the multi-user near-field beamforming optimization problem in a LIS-aided UAV relay system is still an unaddressed research area = [25]–[29].

To address these gaps, this paper focuses on the design of multi-beam near-field beamforming for a multi-user, LIS-aided UAV relay system. Our main contributions are summarized as follows:

Recent research has made significant progress in NF communications and LIS-aided systems. Table I summarizes key related works and highlights the gaps addressed by our study.

This paper fills these gaps. The main contributions of this work are:

- We propose and design two distinct algorithms for this NF-MU problem: a low-complexity Grouped Beamforming heuristic and a high-performance GWO Beamforming metaheuristic.
- To the best of our knowledge, this is the first work to provide a direct and comprehensive comparative analysis of these two approaches, evaluating their effectiveness in an LIS-aided UAV relay system.
- We conduct a thorough scalability analysis (up to $K = 20$ users) and quantify the performance-complexity trade-off, supported by extensive Monte Carlo simulations and statistical tests (Kolmogorov-Smirnov).
- We demonstrate that GWO significantly outperforms in performance (especially fairness, AMAG), but at a substantially higher computational cost ($\approx 300\times$), thereby establishing a clear guideline for algorithm selection in practical deployment scenarios.

II. System Model

We consider a downlink communication scenario as depicted in Fig. 1. A base station (BS) transmits signals to a group of K ground users. Due to potential blockages or long distances, the direct link is unavailable. Instead, the signal is relayed by a high-altitude UAV, which then forwards it to a LIS mounted on a building facade. The LIS, in turn, performs beamforming to serve the K users simultaneously. We focus on the final link from the LIS to the users, which is the most critical part for near-field beamforming.

Within the scope of this research, we focus on designing the near-field beamforming from the LIS to K users under the assumption of a fixed UAV position. Therefore, we assume the UAV operates at a fixed altitude H and a fixed horizontal position $(x_{\text{UAV}}, y_{\text{UAV}})$ during the beamforming phase. The UAV's role here is primarily an Aerial Relay Station (ARS), leveraging its mobility, rapid deployment capabilities, and the ability to establish strong Line-of-Sight (LoS) links to enhance communication efficiency.

In subsequent studies, we will investigate the impact of the UAV's position on the LIS beamforming process to assess the feasibility of joint trajectory and near-field beamforming optimization.

The LIS is a uniform planar array (UPA) of size $M \times N$ located on the $x-y$ plane and centered at the origin $(0, 0, 0)$.

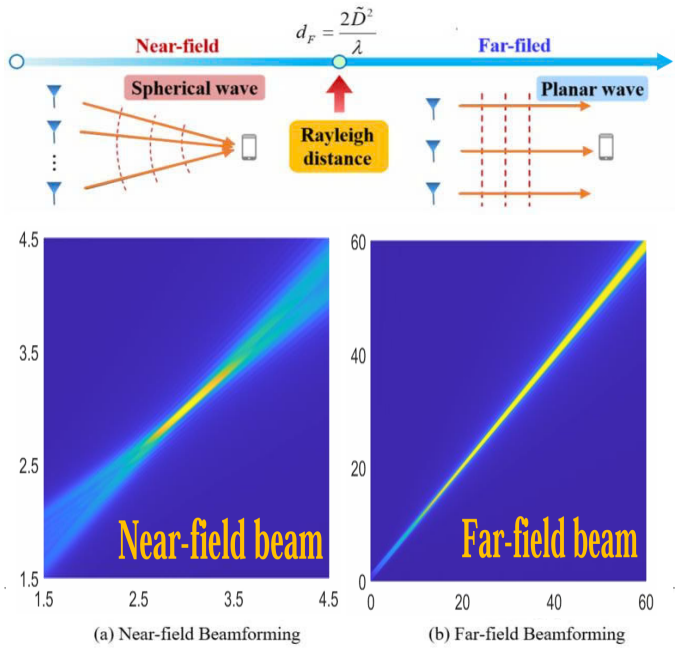

(a) Near-field Beamforming (b) Far-field Beamforming

Fig. 2: Illustration of (a) NF beamforming, where beams are focused to specific points, and (b) FF beamforming, where beams are steered to angles.

The total number of reflecting elements is $N_{\text{LIS}} = MN$. The position of the (m, n)-th element, for $m \in \{1, ..., M\}$ and $n \in \{1, ..., N\}$, is given by:

$$\mathbf{r}_{mn} = \left(\left(m - \frac{M+1}{2} \right) d, \left(n - \frac{N+1}{2} \right) d, 0 \right), \quad (1)$$

where $d = \lambda/2$ is the inter-element spacing and λ is the signal wavelength.

We consider K single-antenna users, with the k-th user located at position $\mathbf{p}_k = (x_k, y_k, z_k)$. The distance from the (m, n)-th LIS element to the k-th user is:

$$d_{k,mn} = \|\mathbf{p}_k - \mathbf{r}_{mn}\|. \quad (2)$$

The key distinction between FF and NF beamforming lies in the modeling of the wavefronts, as illustrated in Fig. 2.

- **FF (Planar Wave Model):** When $d_{k,mn}$ is large, the spherical waves originating from each element can be approximated as planar waves arriving at the user from a specific angle (θ_k, ϕ_k). All rays from the LIS to a single user are parallel.
- **NF (Spherical Wave Model):** When the distance is small, the planar wave approximation is no longer valid. The curvature of the wavefront must be considered, and the rays from different LIS elements arrive at the user from different angles. Beamforming must focus energy onto the specific point $\mathbf{p}_k$.

In practical LIS implementations, phase shifts are typically quantized to B bits, resulting in 2^B discrete levels:

$$\beta_{mn} \in 0, \frac{2\pi}{2^B}, \frac{4\pi}{2^B}, \ldots, (2^B - 1)\frac{2\pi}{2^B}, \quad (3)$$

For analysis in this paper, we first derive algorithms assuming continuous phase shifts ($\beta_{mn} \in [0, 2\pi]$) to establish theoretical performance bounds. The optimal continuous phase β^*_{mn} is then quantized to the nearest discrete level:

$$\beta^q_{mn} = \arg \min_{\beta \in \Phi_B} |\beta - \beta^*_{mn}|, \quad (4)$$

where Φ_B is the set of 2^B discrete phases. This paper analyzes the performance degradation due to quantization for $B = \{1, 2, 3\}$ bits.

The phase shifts to maximize the received signal strength at all K user locations. The coherent array gain for the k-th user, given a set of phase shifts, is calculated as:

$$G_k(\boldsymbol{\beta}) = \left| \sum_{m=1}^{M} \sum_{n=1}^{N} e^{j(\beta_{mn} - \frac{2\pi}{\lambda} d_{k,mn})} \right| \quad (5)$$

The objective is to find $\boldsymbol{\beta}$ that performs well for all users, which we evaluate using the AAG and AMAG:

$$\text{AAG} = \frac{1}{K} \sum_{k=1}^{K} G_k(\boldsymbol{\beta}), \quad (6)$$

$$\text{AMAG} = \mathbb{E}\left[\min_{k \in \{1,\ldots,K\}} G_k(\boldsymbol{\beta}) \right], \quad (7)$$

AMAG is a crucial metric for ensuring fairness among users, averaged over different user position realizations.

Where the expectation is taken over random user positions. In our simulations, users are uniformly distributed within the service area as follows:

$$x_k, y_k \sim ([-10, 10] \text{ m}), \quad z_k \sim ([0.01, 200] \text{ m}),$$

We estimate the AMAG using Monte Carlo sampling with $N_{\text{samples}} = 3300$ realizations:

$$\text{AMAG} \approx \frac{1}{N_{\text{samples}}} \sum_{i=1}^{N_{\text{samples}}} \min_{k \in \{1,\ldots,K\}} G_k(\boldsymbol{\beta}, \mathbf{p}^{(i)}), \quad (8)$$

where $\mathbf{p}^{(i)} = \{\mathbf{p}_1^{(i)}, \ldots, \mathbf{p}_K^{(i)}\}$ denotes the i-th realization of user positions. The 95% confidence interval is computed as

$$\text{CI}_{95} = \text{AMAG} \pm 1.96 \cdot \frac{\sigma_{\text{AMAG}}}{\sqrt{N_{\text{samples}}}}, \quad (9)$$

where σ_{AMAG} is the sample standard deviation.

To comprehensively evaluate the system's performance, rather than only considering instantaneous values, we utilize CDF. The CDF is a statistical tool that provides deep insight into the probability distribution of a random variable. In the context of this paper, the primary random variable is the array gain received by each user.

Mathematically, the CDF of the AAG (or AMAG), denoted as $F_{AG}(x)$, is defined as the probability that the AAG (or AMAG) value for any given user will be less than or equal to a specific threshold value x. The formula is expressed as follows:

$$F_{AG}(x) = P(AG \leq x), \quad (10)$$

Analyzing the CDF curve allows us to visually assess and compare the performance of different algorithms. A CDF curve that is shifted further to the right implies that the system has a higher probability of achieving larger AAG (or AMAG)

values, and therefore, exhibits better overall performance. This provides a quantitative method for understanding the array gain distribution structure, aiding in the prediction and optimization of system performance under various conditions.

III. NEAR-FIELD CHANNEL AND PROPAGATION REGIONS

The distinction between NF and FF is not binary but is characterized by different propagation regions defined by the LIS aperture size and wavelength [9].

A. Field Regions of a LIS

Let $\tilde{D}$ be the largest dimension (diameter) of the LIS, given by:

$$\tilde{D} = \frac{\lambda}{2}\sqrt{(M-1)^2 + (N-1)^2}, \tag{11}$$

The boundary between the radiative NF and the FF is defined by the Fraunhofer distance. in practical scenarios, users are often off-boresight, the Fraunhofer distance is defined as:

$$d_{F,1} = \frac{2\tilde{D}^2}{\lambda}, \tag{12}$$

However, for the ideal case where a user is located on the LIS boresight, the Fraunhofer distance is significantly larger, providing a more conservative boundary:

$$d_{F,2} = \frac{8\tilde{D}^2}{\lambda}. \tag{13}$$

For our 32×32 LIS setup, $d_{F,1} \approx 48.1$ m, while $d_{F,2} \approx 192.2$ m. This large range underscores the high probability of users falling into the NF. The region of primary interest is the Fresnel region, defined for distances $z_k > d_0$ where $d_0 = 8\tilde{D}$. Our proposed algorithms operate under the assumption that users are in this Fresnel region.

B. NF Phase Calculation

In the Fresnel region, the distance $d_{k,mn}$ can be accurately approximated. The optimal phase shift for a single user k at element (m, n) would be $\beta_{mn} = \frac{2\pi}{\lambda} d_{k,mn} \pmod{2\pi}$ to align all signals constructively. The challenge in a MU system is that the optimal phase shift for one user is sub-optimal for all others.

IV. PROPOSED MULTI-USER BEAMFORMING ALGORITHMS

We propose a development path from simple baselines to a low-complexity Grouped beamforming method, and finally to an advanced GWO-based optimization.

A. Baseline 1: FF Beamforming

This is the simplest approach, which completely ignores the NF effects. The phase shifts are set to zero for all elements:

$$\beta_{mn} = 0, \quad \forall m, n. \tag{14}$$

This method serves as a lower bound on performance.

B. Baseline 2: Average Phase Method (AP)

This method is a straightforward extension of single-user FF beamforming. It calculates the FF steering vector for each user k and then sets the LIS phase shifts to the phase of the sum of these vectors. It is still based on the flawed planar wave assumption.

C. Proposed Method 1: Grouped NF Beamforming (Grouped)

The core idea is to partition the $M \times N$ LIS into a grid of smaller, non-overlapping sub-arrays (groups) [9]. All elements within a single group share a common phase shift. Let $\mathcal{G}_{ij}$ be the set of index pairs (m,n) belonging to the group at row i and column j. The optimal phase $\beta_{\mathcal{G}_{ij}}$ for this group is determined as follows:

$$\beta_{\mathcal{G}_{ij}} = \arg\left(\sum_{k=1}^{K} \sum_{(m,n)\in\mathcal{G}_{ij}} e^{-j\frac{2\pi}{\lambda} d_{k,mn}} \right), \tag{15}$$

This calculation is performed independently for each group, finding a compromise phase for all users. The complete procedure is outlined in Algorithm 1.

Algorithm 1 Grouped NF Beamforming

Input: User positions $\{\mathbf{p}_k\}_{k=1}^{K}$, LIS parameters M, N, λ, Group size $S_g \times S_g$
Output: LIS phase shift matrix $\boldsymbol{\beta}$.
Partition the LIS into groups $\mathcal{G}_{ij}$.
for each group $\mathcal{G}_{ij}$ **do**
  Initialize complex sum $C_{sum} = 0$.
  for each user $k = 1, ..., K$ **do**
    Calculate group-user complex vector:
    $V_{k,ij} = \sum_{(m,n)\in\mathcal{G}_{ij}} e^{-j\frac{2\pi}{\lambda}\|\mathbf{p}_k - \mathbf{r}_{mn}\|}$.
    $C_{sum} = C_{sum} + V_{k,ij}$.
  end for
  Calculate the common phase for the group:
  $\beta_{\mathcal{G}_{ij}} = \arg(C_{sum})$.
  Set $\beta_{mn} = \beta_{\mathcal{G}_{ij}}$ for all $(m, n) \in \mathcal{G}_{ij}$.
end for
return $\boldsymbol{\beta}$.

D. Proposed Method 2: GWO NF Beamforming

To improve performance, we propose using the GWO, a powerful metaheuristic algorithm, to find a better set of common phases for the groups.

We select the GWO among various metaheuristic algorithms for the following reasons:

- Superior convergence: GWO demonstrates faster convergence compared and requires fewer tuning parameters than to PSO and GA for multi-modal optimization problems [19],
- Balanced exploration-exploitation: The social hierarchy mechanism (Alpha, Beta, Delta wolves) provides effective balance between global search and local refinement [20],

- Proven success in RIS optimization: Recent work [17] shows GWO's effectiveness for RIS beamforming problems.

Alternative approaches like Semidefinite Relaxation (SDR) or manifold optimization could achieve better performance but with significantly higher computational cost, making them impractical for real-time reconfiguration in UAV-LIS systems.

Algorithm 2 GWO NF Beamforming

Input: User positions $\{\mathbf{p}_k\}_{k=1}^{K}$, LIS parameters, Group size, GWO parameters (population size, max iterations).
Output: LIS phase shift matrix $\boldsymbol{\beta}$.
Partition LIS into groups $\mathcal{G}_i$.
Define the optimization problem for GWO:
    Search space: Group phase vector $\boldsymbol{\Phi}_{\text{grouped}}$.
    Fitness Function: $f(\boldsymbol{\Phi}_{\text{grouped}})$ from Eq. (16).
Initialize GWO: Create a random population of solutions $\boldsymbol{\Phi}_{\text{grouped}}$.
Run GWO optimization loop:
    Calculate fitness for each wolf.
    Identify and save Alpha, Beta, Delta wolves.
    Update positions of other wolves.
Obtain the best solution $\boldsymbol{\Phi}^*_{\text{grouped}}$.
Construct final phase matrix $\boldsymbol{\beta}$ by assigning the optimal phase $\phi^*_{G_i}$ from $\boldsymbol{\Phi}^*_{\text{grouped}}$ to all elements in the corresponding group $\mathcal{G}_i$.
return $\boldsymbol{\beta}$.

1) Problem Formulation: Similar to the Grouped method, the LIS is divided into groups. However, instead of direct calculation, we define the vector of common phases $\boldsymbol{\Phi}_{\text{grouped}} = [\phi_{G_1}, \phi_{G_2}, \ldots, \phi_{G_{N_{\text{groups}}}}]$ as the variable to be optimized. The objective is to find the $\boldsymbol{\Phi}_{\text{grouped}}$ that maximizes the AAG. This becomes the fitness function for GWO:

$$\max_{\boldsymbol{\Phi}_{\text{grouped}}} AAG(\boldsymbol{\Phi}_{\text{grouped}}) = \max_{\boldsymbol{\Phi}_{\text{grouped}}} \frac{1}{K} \sum_{k=1}^{K} G_k(\boldsymbol{\Phi}_{\text{grouped}}) \quad (16)$$

where $G_k(\boldsymbol{\Phi}_{\text{grouped}})$ is defined in (5), with phase shifts determined by the group configuration $\boldsymbol{\Phi}_{\text{grouped}} = [\phi_{G_1}, \phi_{G_2}, \ldots, \phi_{G_{N_{\text{groups}}}}]$.

2) Algorithm Procedure: The GWO Beamforming procedure is outlined in Algorithm 2. It initializes a population of solutions (wolf pack) and iteratively updates their positions based on the three best solutions found so far (Alpha, Beta, and Delta wolves), converging towards a near-optimal solution.

V. SIMULATION RESULTS

This section evaluates the performance of the proposed NF beamforming algorithms through extensive Monte Carlo simulations. We compare our Grouped NF Beamforming (Grouped) and GWO-based Beamforming (GWO) algorithms against two established baselines (FF and AP).

Unless otherwise specified, the simulation parameters are set according to Table II.

Based on the preceding analysis and previous independent simulations, this subsection focuses on comparing the highest-performing configurations. For GWO, we select GWO (2x2) and GWO (8x8), with the latter identified as the best GWO-based approach. For the heuristic method, we select Grouped (2x2), which demonstrated the best fairness, and Grouped (8x8) for a direct comparison. These optimized methods are benchmarked against the FF and AP baselines.

TABLE II: Simulation Parameters

Parameter	Value
LIS size ($M \times N$)	32×32
Wavelength (λ)	0.05 m (6 GHz)
Inter-element spacing (d)	$\lambda/2$
Number of users (K)	5, 10, 20
Number of sampled positions	3300
GWO pack size (population)	30
GWO maximum iterations	256
User x, y range	$[-10, 10]$ m
User z range (distance)	$[0.01, 200]$ m
Fraunhofer distance 1 ($d_{F,1}$)	48.1 m
Fraunhofer distance 2 ($d_{F,2}$)	192.2 m
Fresnel boundary (d_0)	8.8 m

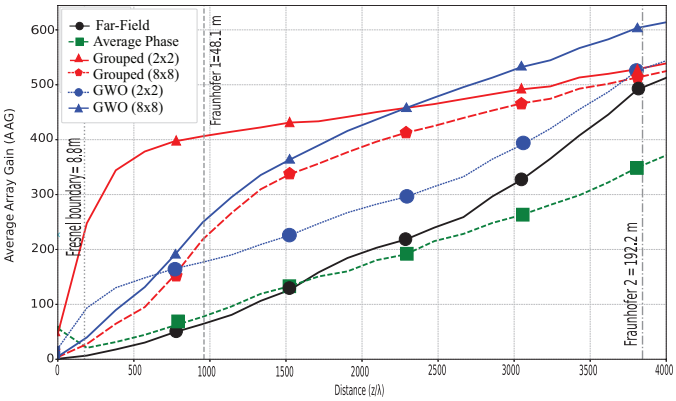

Fig. 3: Average Array Gain (AAG) vs. Normalized Distance for 5 users with all methods.

A. Performance vs. Distance

Fig. 3 and Fig. 4 illustrate the AAG and AMAG performance, respectively, as a function of the normalized distance z/λ. As observed, the GWO-based algorithms, particularly GWO (8x8), consistent outperform all other methods across the entire distance range. In Fig. 3, GWO (8x8) achieves the highest AAG, indicating its superior ability to maximize the total focused energy towards all users. The Grouped (2x2) method also performs well, surpasmsing the baselines, but its gain is noticeably lower than that of GWO.

The fairness performance shown in Fig. 4 is even more telling. GWO (8x8) maintains a significantly higher AMAG compared to all other schemes, confirming its effectiveness in allocating gain equitably among users, even for the worst-case user. This highlights the advantage of the metaheuristic approach in navigating the complex optimization landscape to find a solution that balances the needs of all users. The advantage of GWO becomes much clearer, especially beyond the first Fraunhofer distance. In the extended NF region ($z/\lambda > 2000$), the GWO methods maintain a very high and stable AMAG, ensuring that even the worst-served user receives a high-quality signal. This strongly affirms the superior

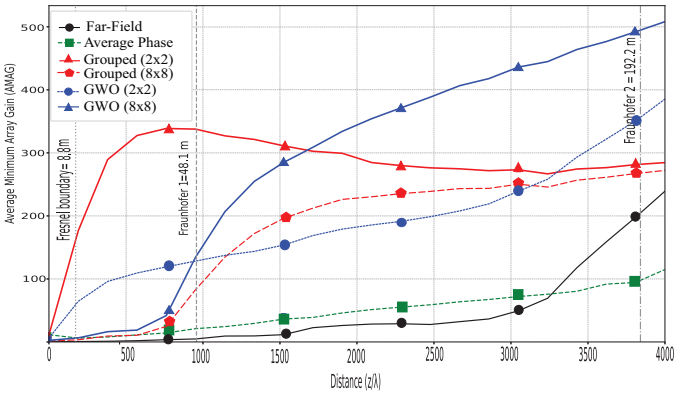

Fig. 4: Average Minimum Array Gain (AMAG) vs. Normalized Distance for 5 users with all methods.

ability of GWO to provide uniform and high-performance service in MU scenarios.

B. Statistical Performance Analysis

The statistical superiority of the GWO algorithm is further validated by the CDF plots for AAG in Fig. 5, respectively.

For $K = 5$ Users (Fig. 5a): In the low user load scenario, the performance differences between algorithms are moderate but statistically significant. The GWO (8×8) configuration demonstrates superior performance in the higher AAG regime (AAG > 450), with approximately 40% of users achieving this level (at CDF $= 0.6$). The performance of grouping methods, particularly the Grouped (2×2) approach, is prominent in the low AAG region (AAG < 320). The baseline methods, Fixed Frequency (FF) and Access Point (AP), show markedly inferior performance, saturating at AAG ≈ 200 for 60% of realizations.

For $K = 10$ Users (Fig. 5b): As user density increases, the performance gap between GWO and heuristic methods widens significantly. The GWO (8×8) CDF curve shifts rightward relative to all other methods, outperforming the Grouped (2×2) strategy in the AAG region of 320 and above (where CDF > 0.5). Conversely, other methods exhibit a leftward shift (performance degradation) as the user count doubles. This suggests that the 8×8 grouping strategy provides an optimal balance between optimization complexity and beamforming flexibility for moderate user loads.

For $K = 20$ Users (Fig. 5c): Under high user density, the superiority of GWO (8×8) becomes most pronounced. The CDF curves show clear separation across the majority of the distribution (CDF > 0.4), with GWO (8×8) consistently achieving 100–150 higher AAG values compared to Grouped (2×2) at equivalent probability levels. Remarkably, even at the 80th percentile, GWO (8×8) maintains AAG > 400, while Grouped (2×2) degrades to AAG ≈ 280. The baseline methods collapse further, with AP and FF barely exceeding AAG $= 200$ for most realizations. This dramatic performance divergence under high user loads validates our hypothesis that metaheuristic optimization becomes increasingly critical as the multi-user interference management problem complexity scales.

C. Fairness Performance Analysis

AMAG Performance show in Fig. 6: The fairness advantage of GWO is starkly evident. In all scenarios, the CDF curves for GWO (8x8) are significantly steeper and located at higher AMAG values. This demonstrates that GWO provides a robust and fair service, ensuring that the worst-case user's performance is substantially elevated. As the user load K increases from 5 to 20, the performance gap between GWO (8x8) and other methods widens, underscoring its scalability and robustness in dense user environments.

For K=5 Users (Fig. 6a): For a low user load, the GWO methods consistently show better performance than their Grouped heuristic counterparts. However, the performance gap is not yet substantial. The benefit from GWO's advanced optimization search is not significant enough to create a breakthrough difference compared to the fast heuristic solution, especially when considering the higher computational complexity of GWO.

For K=10 Users (Fig. 6b): As the number of users increases to 10, the superior performance of the GWO algorithms becomes evident. The CDF curves for GWO methods show a significant shift to the right compared to the Grouped methods. The GWO (8x8) configuration emerges as the most effective solution, clearly outperforming all Grouped configurations. This demonstrates that as the problem becomes more complex, GWO's intelligent search capability proves much more effective than the simple heuristic calculation.

For K=20 Users (Fig. 6c): When the system operates at high load with 20 users, the superiority of the GWO algorithm is most pronounced. The GWO methods, especially GWO (8×8), significantly outperform all Grouped heuristic methods. The CDF curves show a large separation between the two families of algorithms. For instance, at a probability of 80% (CDF$=0.2$), the GWO (8×8) method achieves an AAG above 280, while the best Grouped method struggles to surpass 180. More critically, for AMAG, GWO (8×8) can provide a gain of around 120, effectively doubling the gain of the best Grouped method (approximately 60). This confirms GWO's superior performance in both efficiency and fairness.

The comprehensive statistical analysis—spanning CDF visualizations at standardized comparison points (CDF = 0.5 for AAG, CDF = 0.3 for AMAG), quantitative performance metrics, and rigorous KS hypothesis testing—establishes several key findings in Table III

The performance difference can be explained by the increasing complexity of the optimization space. As K grows, finding a compromise phase configuration becomes significantly more challenging due to the larger search space and increased inter-user interference. The simple averaging of the Grouped heuristic is no longer sufficient. In contrast, GWO's global search capability allows it to effectively explore this complex solution space and find a balanced phase configuration that benefits the entire user group. The GWO (8x8) configuration consistently performs best because it strikes an optimal balance: its 16 optimization variables create a search space small enough for GWO to explore effectively, while the 8x8 group size remains flexible enough to shape high-quality focused beams.

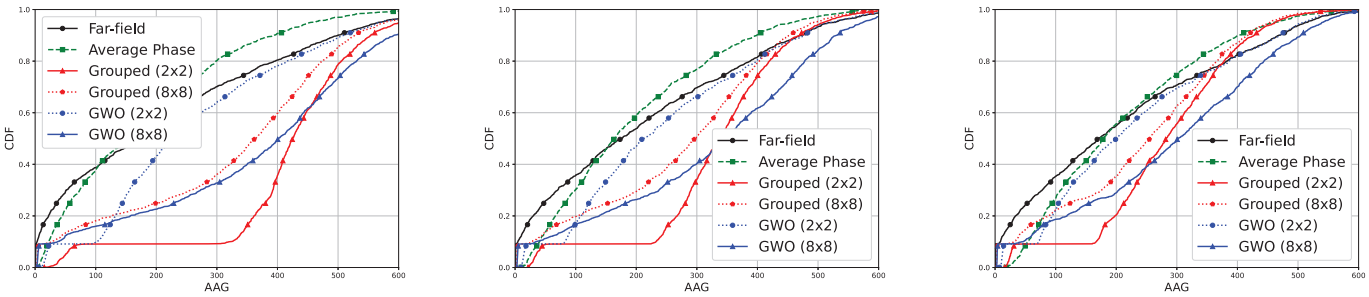

(a) $K = 5$ Users (b) $K = 10$ Users (c) $K = 20$ Users

Fig. 5: CDF of AAG for different numbers of users with all methods.

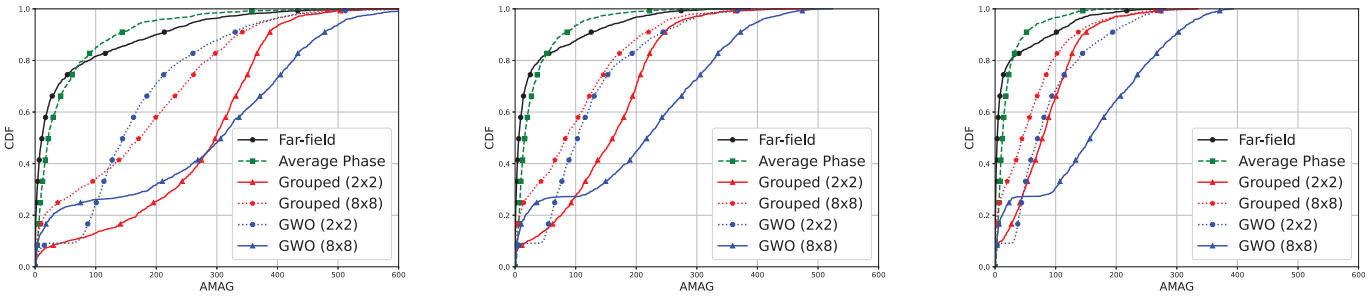

(a) $K = 5$ Users (b) $K = 10$ Users (c) $K = 20$ Users

Fig. 6: CDF of AMAG for different numbers of users with all methods.

TABLE III: Performance Comparison at Standardized CDF Reference Points

Metric	Method	K=5	K=10	K=20	Winner
AAG (CDF=0.5)	FF	180	170	160	–
	AP	150	160	170	–
	Grouped (2×2)	**420**	320	280	K≤5
	GWO (8×8)	400	**350**	**300**	K>5
AMAG (CDF=0.3)	FF	10	5	3	–
	AP	14	12	10	–
	Grouped (2×2)	**230**	120	50	K≤5
	GWO (8×8)	200	**155**	**100**	K>5
Performance Improvement (GWO vs Grouped):					
AAG Improvement		-5%	+9%	+7%	Crossover at K≈5-7
AMAG Improvement		-13%	+24%	+50%	Crossover at K≈5-7

Note: CDF=0.5 represents median (50% achieve this or better); CDF=0.3 represents 70th percentile (70% achieve this or better). **Bold** values indicate best performance for each user load. Negative improvement indicates heuristic superiority at low load.

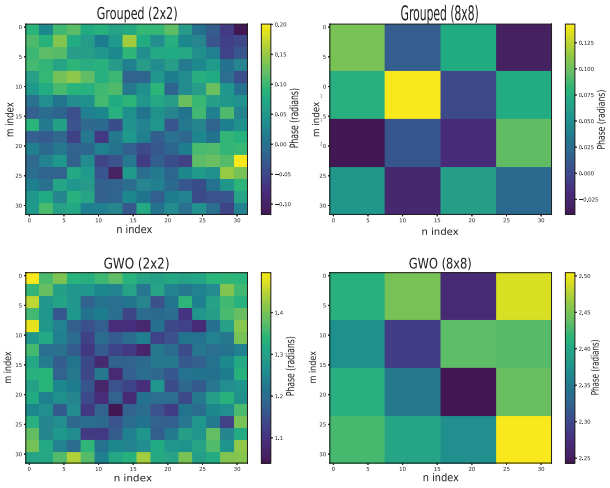

Fig. 7: Average phase heatmaps for 20 users comparing GWO and Grouped methods, averaged over multiple simulations.

D. LIS Phase Configuration Analysis (Heatmaps Phase)

Fig. 7 illustrates the average phase values of the LIS elements, averaged over multiple simulation samples with varying UE positions. This plot not only shows instantaneous phase values but also reflects the long-term stability trend and statistical convergence of the phase configuration. From this, we can assess the stability and average phase dispersion over many simulation runs, thereby gaining a better understanding of the sustainability of the optimal solution.

Heatmap for the Grouped algorithm: Previous results have shown that the Grouped (2x2) offers superior performance among the Grouped methods and when compared to the FF and AP methods. The heatmap for this configuration will reveal how the resolution of sub-array division significantly impacts system performance, suggesting that a finer subdivision tends to increase system efficiency.

Heatmap for the GWO methods: In contrast, while the GWO (8x8) configuration, which ultimately leads in performance, has a much simpler heatmap than GWO (2x2), it has demonstrated superiority over all Grouped, FF, and AP methods, particularly in scenarios with a large number of users (e.g., K=20). The heatmap for GWO (8x8) illustrates its ability to find an optimal phase configuration for a complex MU environment, ensuring efficient energy distribution to all UEs. This highlights the balance between system performance and the computational complexity inherent in Metaheuristic algorithms. Selecting an appropriate group size is crucial for reducing the computational load, thereby avoiding the "curse of dimensionality" or "overfitting". The fact that the GWO 8x8 configuration yielded the best results in our initial simulations carries significant practical importance: it has identified the optimal "sweet spot" between solution quality and computational cost.

E. Computational Complexity Analysis

The superior performance demonstrated by the GWO algorithm comes at a quantifiable computational cost, as detailed in Table IV. The GWO (8x8) configuration requires approximately 2400 ms per optimization cycle on the test platform (Intel i7-10700K, 64 GB RAM, Python 3.10.11). This runtime is significantly higher—roughly 300 times longer—than the 8 ms required by the Grouped (2x2) heuristic. This difference stems directly from their algorithmic complexities: GWO operates iteratively with a complexity of $\mathcal{O}(T \cdot P \cdot K \cdot MN)$, involving 7,680 fitness evaluations (256 iterations $\times$ 30 population size) in our setup. In contrast, the Grouped heuristic performs a single-pass calculation with linear complexity $\mathcal{O}(K \cdot MN)$. The baseline methods (FF and AP) exhibit negligible or linear complexity, resulting in near-instantaneous runtimes ($<$5 ms). This stark contrast highlights the fundamental trade-off between computational overhead and achievable performance gains when selecting beamforming strategies.

TABLE IV: Computational complexity and runtime comparison (measured on Intel i7-10700K, 64 GB Ram, Python 3.10.11)

Method	**Complexity**	**Runtime (ms)**	**Scalability**
FF	$\mathcal{O}(1)$	< 1	Excellent
AP	$\mathcal{O}(K \cdot MN)$	5	Good
Grouped (2×2)	$\mathcal{O}(K \cdot MN)$	8	Good
Grouped (8×8)	$\mathcal{O}(K \cdot MN)$	12	Good
GWO (8×8)	$\mathcal{O}(T \cdot P \cdot K \cdot MN)$	2400	Limited

VI. Conclusions

In this paper, we conducted a comprehensive investigation and comparative analysis of the performance of two primary phase configuration algorithms—a low-complexity Grouped Beamforming heuristic and a GWO Beamforming metaheuristic for a MU LIS-UAV communication system operating in the NF region.

The simulation results, validated by Kolmogorov-Smirnov statistical tests, reveal distinct performance characteristics. The Grouped Beamforming algorithm, particularly the (2x2) configuration, offers a substantial improvement over baseline FF and AP methods and presents a computationally efficient solution suitable for low-latency requirements. However, its effectiveness, especially in ensuring user fairness (AMAG), diminishes notably under higher user loads (K=10 and K=20). Conversely, the GWO algorithm, optimized with an (8x8) grouping, consistently demonstrates superior performance across all evaluated metrics. It achieves significantly higher AAG and, critically, doubles the AMAG compared to the best Grouped method in the challenging K=20 scenario, showcasing its robustness and ability to maintain fairness by effectively exploring the complex solution space, as visually suggested by the resulting phase heatmaps.

This work's unique contribution lies in quantifying the fundamental performance complexity trade-off inherent in these NF beamforming strategies for the LIS-UAV context (Table IV). While GWO delivers superior gains, its computational runtime is approximately 300 times higher than the Grouped heuristic (2400 ms vs. 8 ms). This establishes a clear design guideline: the low-complexity Grouped Beamforming is well-suited for dynamic environments demanding real-time phase adaptations (e.g., latency $<$ 10 ms), whereas the high-performance GWO algorithm is the preferred choice for semi-static scenarios (e.g., hovering UAV relay) where maximizing system throughput and user fairness is paramount, and periodic optimization is feasible.

Future research directions will extend this work in several key ways:

1) Joint Optimization: Integrate UAV trajectory design with the GWO beamforming algorithm for the LIS to jointly optimize the relay's position and the NF phase configuration, potentially using reinforcement learning techniques.
2) Realistic Channel and Hardware Models: Evaluate the algorithms' performance under more practical conditions, incorporating factors like hardware impairments (e.g., phase noise, mutual coupling), imperfect channel state information (CSI) acquisition, and the impact of additive noise across different SNR regimes.
3) Quantization and Scalability: Analyze the performance degradation resulting from discrete phase shifters (e.g., 1-3 bits quantization) commonly used in practical LIS implementations and further investigate the scalability of both heuristic and metaheuristic approaches for even larger LIS dimensions (e.g., 64x64 arrays) and varying user distributions.

References

[1] W. M. Othman, A. A. Ateya, M. E. Nasr, A. Muthanna, M. ElAffendi, A. Koucheryavy, and A. A. Hamdi, "Key enabling technologies for 6g: The role of uavs, terahertz communication, and intelligent reconfigurable surfaces in shaping the future of wireless networks," *Journal of Sensor and Actuator Networks*, vol. 14, no. 2, 2025. [Online]. Available: https://www.mdpi.com/2224-2708/14/2/30

[2] H. Tataria, M. Shafi, A. F. Molisch, M. Dohler, H. Sjöland, and F. Tufvesson, "6g wireless systems: Vision, requirements, challenges, insights, and opportunities," *Proceedings of the IEEE*, vol. 109, no. 7, pp. 1166–1199, 2021. doi: 10.1109/JPROC.2021.3061701 .

[3] Z. Wang, J. Zhang, H. Du, W. E. I. Sha, B. Ai, D. Niyato, and M. Debbah, "Extremely large-scale mimo: Fundamentals, challenges, solutions, and future directions," *IEEE Wireless Communications*, vol. 31, no. 3, pp. 117–124, 2024. doi: 10.1109/MWC.132.2200443 .

[4] J. An, C. Yuen, L. Dai, M. Di Renzo, M. Debbah, and L. Hanzo, "Near-field communications: Research advances, potential, and challenges," *IEEE Wireless Communications*, vol. 31, no. 3, pp. 100–107, 2024. doi: 10.1109/MWC.004.2300450 .

[5] M. D. Renzo, M. Debbah, D.-T. Phan-Huy, A. Zappone, M.-S. Alouini, C. Yuen, V. Sciancalepore, G. C. Alexandropoulos, J. Hoydis, H. Gacanin, J. de Rosny, A. Bounceu, G. Lerosey, and M. Fink, "Smart radio environments empowered by ai reconfigurable meta-surfaces: An idea whose time has come," 2019. [Online]. Available: https://arxiv.org/abs/1903.08925

[6] Y. Zeng, R. Zhang, and T. J. Lim, "Wireless communications with unmanned aerial vehicles: opportunities and challenges," *IEEE Communications Magazine*, vol. 54, no. 5, pp. 36–42, 2016. doi: 10.1109/MCOM.2016.7470933 .

[7] Y. Zhang, G. Wang, S. Peng, Y. Leng, G. Yu, and B. Wang, "Near-field beamforming algorithms for uavs," *Sensors*, vol. 23, no. 13, 2023. [Online]. Available: https://www.mdpi.com/1424-8220/23/13/6172

[8] "Beamforming design and trajectory optimization for learning-based multi-uav-assisted integrated sensing and communication systems," *Computer Networks*, vol. 273, p. 111751, 2025. doi: https://doi.org/10.1016/j.comnet.2025.111751 .

[9] S. Hu, H. Wang, and M. C. Ilter, "Design of near-field beamforming for large intelligent surfaces," *IEEE Transactions on Wireless Communications*, vol. 23, no. 1, pp. 762–774, 2024. doi: 10.1109/TWC.2023.3281885 .

[10] V. Sharma, N. Garg, S. Sharma, and V. Bhatia, "A mini-review of signal processing techniques for ris-assisted near field thz communication," *Frontiers in Signal Processing*, vol. Volume 3 - 2023, 2024. [Online]. Available: https://www.frontiersin.org/journals/signal-processing/articles/10.3389/frsip.2023.1297945

[11] M. Cui, Z. Wu, Y. Lu, X. Wei, and L. Dai, "Near-field communications for 6g: Fundamentals, challenges, potentials, and future directions," *IEEE Communications Magazine*, vol. PP, pp. 1–7, 01 2022. doi: 10.1109/MCOM.004.2200136 .

[12] Z. Wang, X. Mu, Y. Zou, and Y. Liu, "Near-field wideband beamfocusing optimization: A heuristic two-stage approach," in *GLOBECOM 2023 - 2023 IEEE Global Communications Conference*, 2023, pp. 783–788. doi: 10.1109/GLOBECOM54140.2023.10437679 .

[13] S. Xue, J. Zhao, X. Mu, K. Cai, Z. Yanbo, and Y. Liu, "Near-field beamforming with 3d velocity sensing and localization for uav communications," 03 2025, pp. 1–6. doi: 10.1109/WCNC61545.2025.10978527 .

[14] W. Liu, C. Pan, H. Ren, J. Wang, R. Schober, and L. Hanzo, "Near-field multiuser beam-training for extremely large-scale mimo systems," 2024.

[15] Z. Wang, X. Mu, and Y. Liu, "Performance bounds of near-field sensing with circular arrays," in *GLOBECOM 2024 - 2024 IEEE Global Communications Conference*, 2024, pp. 2767–2772. doi: 10.1109/GLOBECOM52923.2024.10901613 .

[16] K. Singh, H. Albinsaid, S. Singh, C. Pan, and S. Biswas, "Drl-based beamforming design in ris-aided multi-user wireless networks," 12 2023, pp. 224–229. doi: 10.1109/ANTS59832.2023.10469394 .

[17] A. N. Soumana Hamadou, C. Wa Maina, and M. Moindze Soidridine, "A grey wolf optimiser (gwo)-based ris phase shift design for a ris-assisted multi-antenna system," *IEEE Communications Letters*, vol. 28, no. 9, pp. 2171–2175, 2024. doi: 10.1109/LCOMM.2024.3423013 .

[18] M. Bakhshi, S. Bayat, and R. Amiri, "Optimal ris placement in near-field localization using gray wolf optimizer," *IEEE Transactions on Vehicular Technology*, vol. 74, no. 4, pp. 6795–6800, 2025. doi: 10.1109/TVT.2024.3520232 .

[19] "Grey wolf optimizer," *Advances in Engineering Software*, vol. 69, pp. 46–61, 2014. doi: 10.1007/978-981-10-5221-7_9 .

[20] A. Issa, A. Daghal, and A. Sallomi, "A beamforming study of the linear antenna array using grey wolf optimization algorithm," *Indonesian Journal of Electrical Engineering and Computer Science*, vol. 20, pp. 1538–1546, 12 2020. doi: 10.11591/ijeecs.v20.i3.pp1538-1546 .

[21] R. Tota, M. S. Hossain, M. Z. Sultan, and H. Roni, "Robust near-field circular beamformer with artificial intelligence based side-lobe reduction technique," *Circuits, Systems, and Signal Processing*, vol. 43, pp. 7139–7172, 07 2024. doi: 10.1007/s00034-024-02785-0 .

[22] L. Yang, D. Guo, Y. Liu, and L. Feng, "Joint trajectory and power optimization for uav-assisted communication networks," in *2024 10th International Conference on Computer and Communications (ICCC)*, 2024, pp. 2542–2547. doi: 10.1109/ICCC62609.2024.10941717 .

[23] M. Qian, X. Mu, L. You, and M. Matthaiou, "Near-field multi-user holographic mimo communications over ricean fading channels," in *2025 IEEE Wireless Communications and Networking Conference (WCNC)*, 2025, pp. 1–6. doi: 10.1109/WCNC61545.2025.10978499 .

[24] N. Xue, X. Mu, Y. Chen, and Y. Liu, "Near-field isac for a ris-assisted system," in *GLOBECOM 2024 - 2024 IEEE Global Communications Conference*, 2024, pp. 4034–4039. doi: 10.1109/GLOBECOM52923.2024.10901485 .

[25] G. Zhu, X. Mu, L. Guo, A. Huang, and S. Xu, "Large-scale star-ris assisted mixed near- and far-field swipt," 12 2024, pp. 3769–3774. doi: 10.1109/GLOBECOM52923.2024.10901343 .

[26] H. Li, X. Mu, Y. Liu, Y. Chen, and Z. Pan, "Joint beamforming design for star-ris aided cognitive radio systems," in *GLOBECOM 2024 - 2024 IEEE Global Communications Conference*, 2024, pp. 2906–2911. doi: 10.1109/GLOBECOM52923.2024.10901748 .

[27] R. Zhong, X. Mu, M. Jaber, and Y. Liu, "A mobile edge generation approach," in *GLOBECOM 2024 - 2024 IEEE Global Communications Conference*, 2024, pp. 4173–4178. doi: 10.1109/GLOBECOM52923.2024.10901654 .

[28] J. Lei, X. Mu, T. Zhang, and Y. Liu, "Noma for td-stars assisted thz wideband multi-user communications," in *2024 IEEE Globecom Workshops (GC Wkshps)*, 2024, pp. 1–6. doi: 10.1109/GCWkshp64532.2024.11101588 .

[29] M. B. Yilmaz, L. Xiang, and A. Klein, "Joint beamforming and trajectory optimization for uav-enabled isac under a finite energy budget," in *2024 IEEE International Conference on Communications Workshops (ICC Workshops)*, 2024, pp. 1876–1881. doi: 10.1109/ICCWorkshops59551.2024.10615353 .